Chapter 13

Adjacent seas of the Indian Ocean and the Australasian Mediterranean Sea (the Indonesian throughflow)

Being the smallest of all oceans, the Indian Ocean does not have the large number of distinct subregions found in the Pacific and Atlantic Oceans. Regions known under their own names include the Bay of Bengal and the Arabian Sea already discussed in the previous chapter, the Mozambique Strait (mentioned in the discussion of the western boundary currents), and the Great Australian Bight, clearly the least researched part of the Indian Ocean. Malacca Strait and the Andaman Sea form the transition region between the Bay of Bengal and the adjacent seas of the Pacific Ocean in Southeast Asia. The only regional seas that have some impact on the hydrography of the Indian Ocean and therefore require separate discussion are the Red Sea and the Persian Gulf. Since that discussion will not provide sufficient material for a full-length chapter, we include here the description of the Australasian Mediterranean Sea and what is often known as the Indonesian throughflow, i.e. the exchange of water between the Pacific and Indian Oceans. The Australasian Mediterranean Sea is of course a regional sea of the Pacific Ocean; but its impact on the Indian Ocean is much bigger than its influence on Pacific hydrography, and its inclusion in this chapter is justified on that ground alone.

The Red Sea

The Red Sea can be considered the prototype of a concentration basin. It is a deep mediterranean sea with a relatively shallow sill in a region where evaporation vastly exceeds precipitation (evaporation 200 cm per year, rainfall 7 cm per year, giving a net annual water loss of nearly 2 m). In such a basin water entering from the ocean in the surface layer undergoes a salinity increase and gets denser as it flows towards the inner end of the sea. This provokes vertical convection and guarantees continuous renewal of the water in the lower layer, which eventually leaves the basin in an undercurrent over the sill.

Geologically, the Red Sea is a rift valley formed during the separation of Africa and Arabia. Its topography (Figure 13.1) shows a maximum depth near 2900 m and a sill depth of about 110 m, significantly less than the average depth of 560 m. It is about 2000 km long but on average only 250 km wide. At its northern end it includes the shallow Gulf of Suez with average depths between 50 - 80 m and the Gulf of Aqaba, a smaller version of the Red Sea itself with a maximum depth near 1800 m and a sill depth close to 300 m.

Figure 13.2 gives a hydrographic section along the axis of the Red Sea and into the Gulf of Suez. The most notable feature is the extremely high salinity which makes the Red Sea the most saline region of the world ocean and gives it the character of an inverse estuary. The long and narrow shape of the basin isolates the inner part from direct exchange with the open ocean, so surface salinity increases continuously from 36 at the Strait of Bab el Mandeb to above 40 in the interior. Highest salinities above 42 are attained in the northern Red Sea and the shallow Gulf of Suez. In both regions the winter months, when the sea surface temperature in the Gulf of Suez sinks below 20°C (it ranges between 27 - 30°C

Fig. 13. Topography of the Red Sea. *DD* marks the Discovery Deep, the depression where the first observations of hot brines were made. Arrows indicate prevalent wind directions for summer (full arrows) and winter (open arrows). Depths are in m.
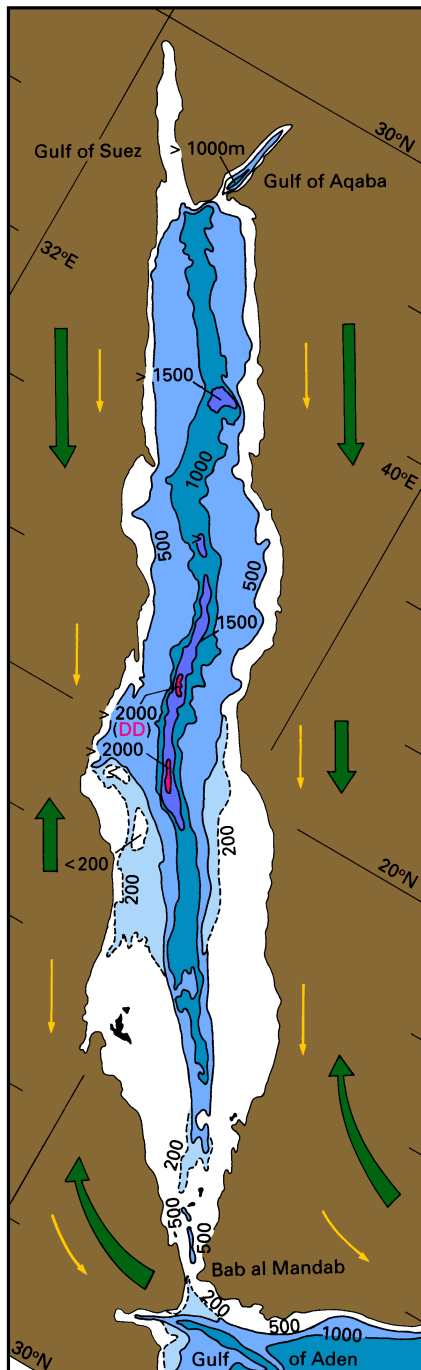
during summer), are a period of active convection. Which of the two regions is responsible for the formation of deep water has been a matter of debate for many years. Recent observations of bomb radiocarbon indicate that both contribute, but in different ways. The winter water from the Gulf of Suez is very dense; it falls down the continental slope and fills the depths of the Red Sea below 1000 m. When the water starts its descent it has a temperature below 18°C and a salinity above 42; but mixing quickly modifies this, and the water soon ends up with the standard Red Sea deep water properties of 21.5°C and 40.6 salinity. Winter water from the northern Red Sea is slightly less dense; it slides down on the appropriate isopycnal surface and spreads below the surface mixed layer. The resulting circulation is indicated in Figure 13.2. A lower circulation cell with slow upward movement, gradual loss of oxygen, and a northward return flow at its upper limit is capped by southward movement of water from the second source. This is reflected in an oxygen minimum below the thermocline, indicating that the oldest water is at the top of the

Fig. 13.2. Hydrographic section along the axis of the Red Sea, winter conditions.

(a) Potential temperature (°C)

(b) salinity

(c) oxygen (ml/l).

Arrows indicate the flow of deep water as derived in Cember (1988).

lower circulation cell. It is worth noting that even at the oxygen minimum, Red Sea Water has a higher oxygen content than the very old Indian Central Water found at the same depth in the Indian Ocean thermocline; consequently, east of Bab el Mandeb Red Sea Water manifests itself through an oxygen maximum. Oxygen values in the 150 - 200 m thick surface layer of the Red Sea correspond to saturation values, which at these high temperatures are relatively low (less than 4 ml/l in summer).

Estimates for the residence time of deep water are just as controversial as identification of its sources and vary from a few years to two centuries. Recent radiocarbon data indicate a residence time slightly less than 40 years. This is the best available estimate at present.

The outflow of Red Sea water into the Arabian Sea is clearly visible in Figure 13.2, most prominently in salinity. It is seen that the dense water flows down the continental slope to a depth of 1500 m and more; but the bulk of the water is modified by mixing soon after passing Bab el Mandeb and spreads between 500 - 1000 m with a temperature of 13 - 14°C and a salinity of 36.5 or less. The magnitude of the outflow at Bab el Mandeb is quite small. Measurements during the summer of 1982 indicated only 0.25 - 0.3 Sv; similar observations over a few months in 1965 showed intermittent outflow of about 0.5 Sv depending on the direction of the wind. Nevertheless, the concentration of salt in the outflow is sufficient to guarantee that Red Sea Water can be traced in the Indian Ocean thermocline even into the southern hemisphere, as we saw in the last chapter.

Seasonal variations in the outflow are related to the monsoons, which determine the surface circulation in the Red Sea in general. Winds over the Red Sea form part of the general monsoon system of the Indian Ocean but are modified by the influence of the land, which establishes a belt of low air pressure from Asia towards northern Africa during summer and a centre of high pressure over northern Africa during winter. The resulting pressure gradients against the region of constant air pressure in the tropics produce northwesterly winds throughout the year north of 20°S. South of that latitude winds are from the northwest during summer but reverse to southeasterly during winter. Throughout the entire region winds are generally stronger in winter than in summer. The resulting flow is northward in winter, south of 20°S under the direct forcing of the wind which supports surface inflow through Bab el Mandeb, further north driven by the sinking of surface water even though winds north of 20°S are predominantly from the northwest. In summer the wind opposes surface inflow, but during most of the time its strength is insufficient to suppress the surface inflow necessary to maintain the water budget. Occasionally water movement at the surface is southward and inflow occurs intermittently at intermediate depths. It is estimated that the water stays in the upper layer circulation for about 6 years before sinking.

A remarkable feature of the Red Sea is the extremely high water temperature and salinity found in various depressions of the sea floor (Figure 13.3). This is the result of geothermal heating through vents in the ocean crust, which brings minerals contained in the crust and in the sediment into solution. The resulting brine is dense enough to remain at the ocean floor even at very high temperatures. Values close to 58°C have been recorded, together with "salinities" in excess of 300. The salinity readings were obtained by diluting brine samples until their salinity came into the range of normal CTD instruments. Such determinations are invariably incorrect since the universal rule that the relative composition of sea salt remains the same throughout the world ocean does not hold in brines brought up from fissures in the earth's crust - the content in metal ions is much higher than in the

normal salinity mix. Gravimetric salinity determinations (weighing the sample before and after evaporation of the water) are more accurate; they still give salinities in excess of 250.

The Red Sea was the first region where hot brines were discovered at the sea floor (Figure 13.1). Similarly high temperatures and salinities are now known to exist above fissures in mid-ocean ridges of other ocean regions; temperatures in excess of 320°C have been measured at hydrothermal vents in the Pacific Ocean. More commonly, vents are associated with seepage of hypersaline water at environmental temperatures; this is the case for the majority of vents in the Pacific Ocean and those reported from the Gulf of Mexico. Large brine deposits can only accumulate where such vents are located in topographic depressions. The deposits in the Red Sea are possibly large enough to warrant commercial metal extraction at some time in the future.
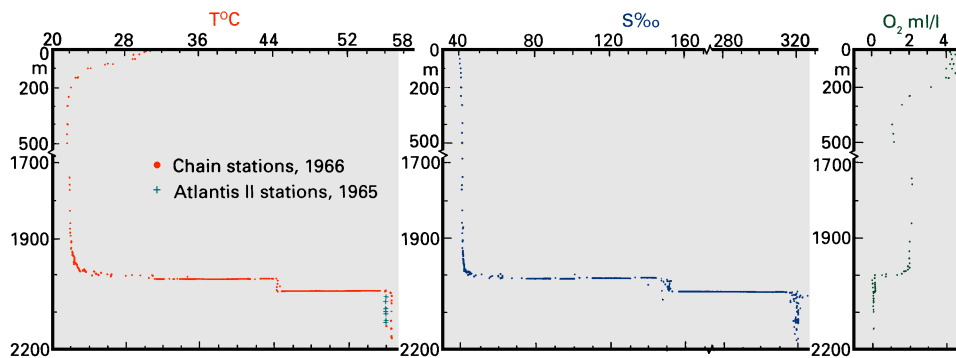
Fig. 13.3. Temperature and "salinity" (see explanation in text) in a hydrothermal vent of the Red Sea. From Brewer *et al*. (1969).

The Persian Gulf

The hydrography of the Persian Gulf is very similar to that of the Red Sea; but the much smaller volume of the Persian Gulf greatly reduces its impact on the Indian Ocean. Its length of 800 km together with an average width of 200 km gives it an area comparable to that of the Red Sea. Atmospheric conditions do not differ much between the two mediterranean seas (except that winds are from the north or northeast throughout the year over the entire area). The Persian Gulf is therefore a concentration basin, too. The rate of water loss at the surface is only slightly reduced by river runoff from the Euphrates and Tigris rivers. The main difference is that the Persian Gulf belongs entirely to the continental shelf, has a mean water depth of only 25 m and, with a sill depth at the Strait of Hormuz only marginally above its average depth, cannot hold back large quantities of salty deep water.

Figure 13.4 gives a hydrographic section through the Persian Gulf and the adjoining part of the Arabian Sea. Despite the difference in volume and residence time, the waters entering the Indian Ocean from the Persian Gulf and the Red Sea have very similar characteristics. The major difference is in oxygen content, which is markedly higher in Persian Gulf Water

because the residence time is much shorter. Since Indian Central Water near the Strait of Hormuz is older and its oxygen content lower than at Bab el Mandeb, the oxygen maximum produced by the outflowing water is even more marked. Persian Gulf Water also tends to have somewhat lower density than Red Sea Water (on account of its higher temperature) and therefore tends to stay above the main thermocline rather than penetrating it. Nevertheless, at some distance from the Strait of Hormuz it is often difficult to separate traces of Red Sea and Persian Gulf Water, and the two water masses are often regarded as one.
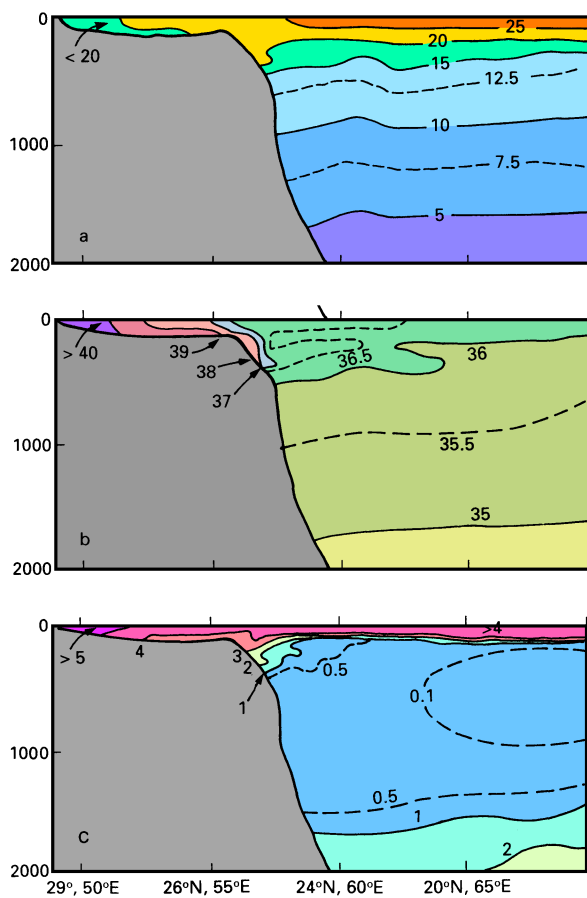
Fig. 13.4. Hydrographic section along the axis of the Persian Gulf, winter conditions

(a) Potential temperature (°C)

(b) salinity,

(c) oxygen (ml/l).

The Australasian Mediterranean Sea and the Indonesian throughflow

Of all the regional seas of the world ocean, the Australasian Mediterranean Sea displays without doubt the most complicated topography. It consists of a series of very deep basins with very limited interconnections, each basin being characterized by its own variety of bottom water. The exact number of deep basins found within its borders is difficult to define; most nautical charts usually recognize at least eight basins under their own name
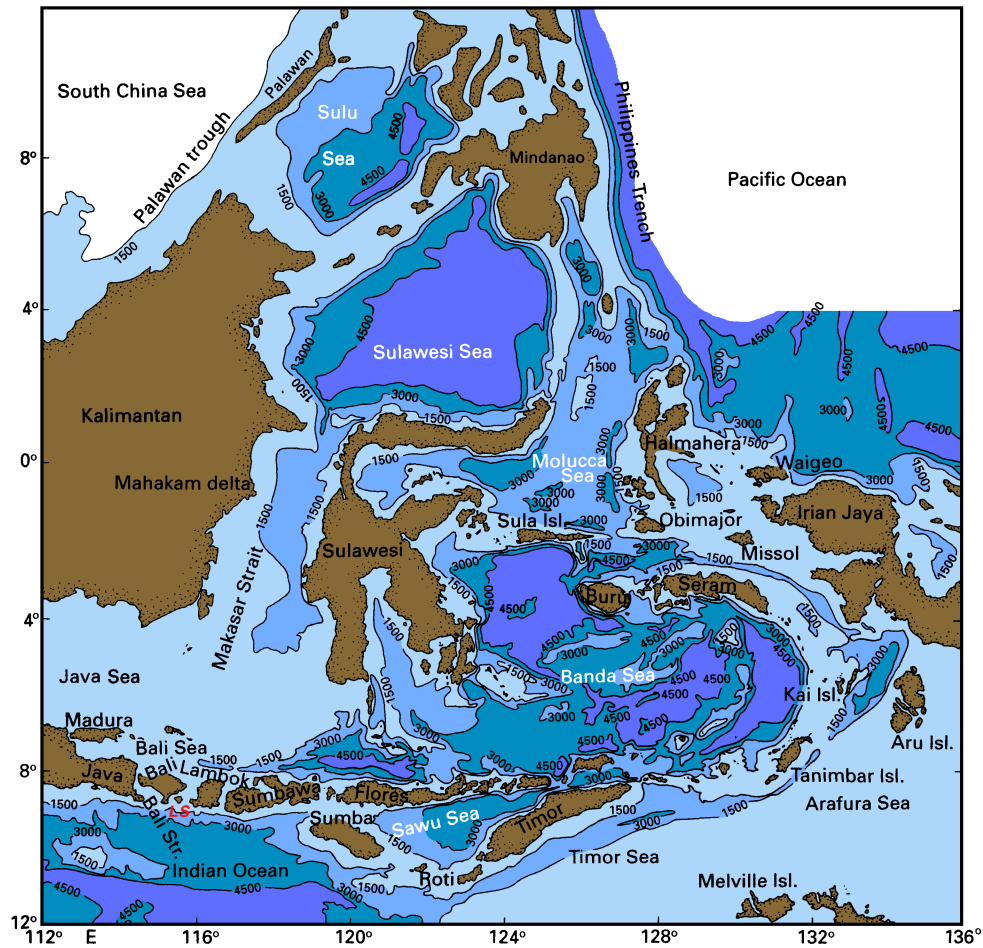
Fig. 13.5. Topography of the Australasian Mediterranean Sea. Depths are in m. LS: Lombok Strait.

(Figure 13.5). The largest and deepest is the Banda Sea which has depths in excess of 4500 m in the southeast (also known as the South Banda Sea) and in the northwest (the North Banda Sea), separated by a ridge of less than 3000 m depth; largest depths are near 7440 m in the south and 5800 m in the north. The Sulawesi Sea (formerly known as the Celebes Sea) is a single basin of similar size deeper than 5000 m over most of its area. Between these two major basins are three basins deeper than 3000 m, the Molucca, Halmahera, and Seram Seas, the latter being deeper than 5300 m. North of the Sulawesi Sea and enclosed by the islands of the Philippines is the Sulu Sea, which has depths in excess of 4500 m. The Flores Sea is located in the south, connecting the Banda Sea with the shallow Java Sea and reaching nearly 6400 m in a deep depression. The Sawu Sea, which reaches nearly 3500 m depth, is the southernmost basin between Timor, Sumba, and Flores. Another important topographic feature is Makassar Strait between the Sulawesi and
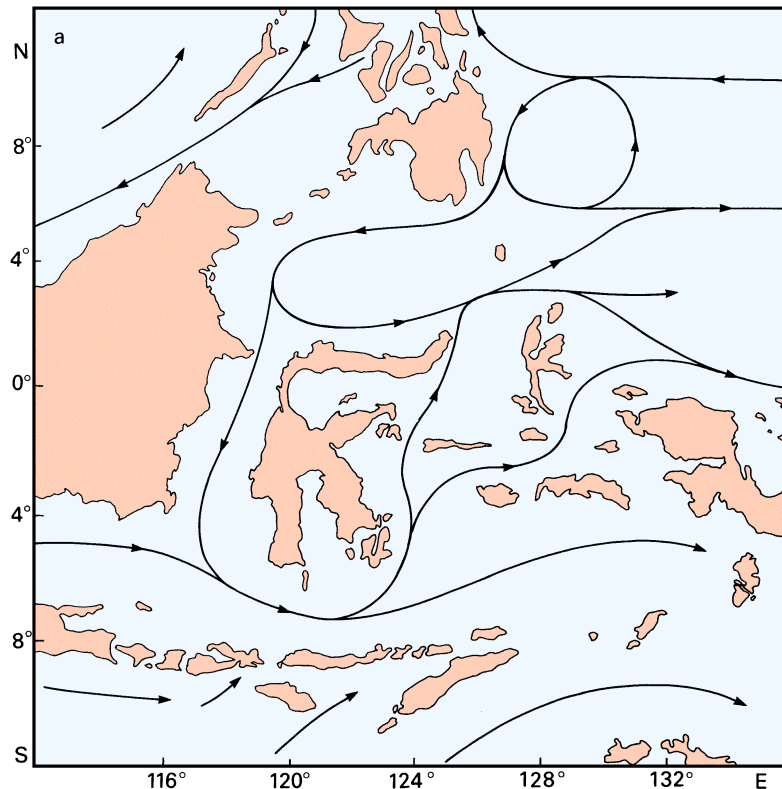
Fig. 13.6. Surface currents in the Australasian Mediterranean Sea. (a) In February (north monsoon, minimum throughflow), (b, page 223) in August (south monsoon, maximum throughflow).

Java Seas; it is shallow in the west but over 2000 m deep in the east where it is connected without obstruction to the Sulawesi Sea in the north.

The climate of the Australasian Mediterranean Sea is characterized by monsoonal winds and high rainfall. Winds blow from the south, curving across the equator with a westward component in the south and an eastward component in the north, during May - September and in nearly exactly the opposite direction during November - March (Figure 1.2). Rain occurs at all times of the year and exceeds 400 cm in the annual mean near the junction of the Intertropical and South Pacific Convergences. As in the western equatorial Pacific Ocean, it is released from strong localized convection cells that are only a few kilometers in diameter, reach high into the upper atmosphere, and are surrounded by cloud-free regions of sinking air. As a consequence, solar heat input over the Australasian Mediterranean Sea is high (Figure 1.5) despite relatively high cloud-cover (Figure 8.5). Evaporative heat loss is high on account of high sea surface temperatures; but on balance the ocean receives more heat than is lost to the atmosphere. There is also more freshwater gain than evaporation, and the *P-E* balance (Figure 1.7) is strongly positive.
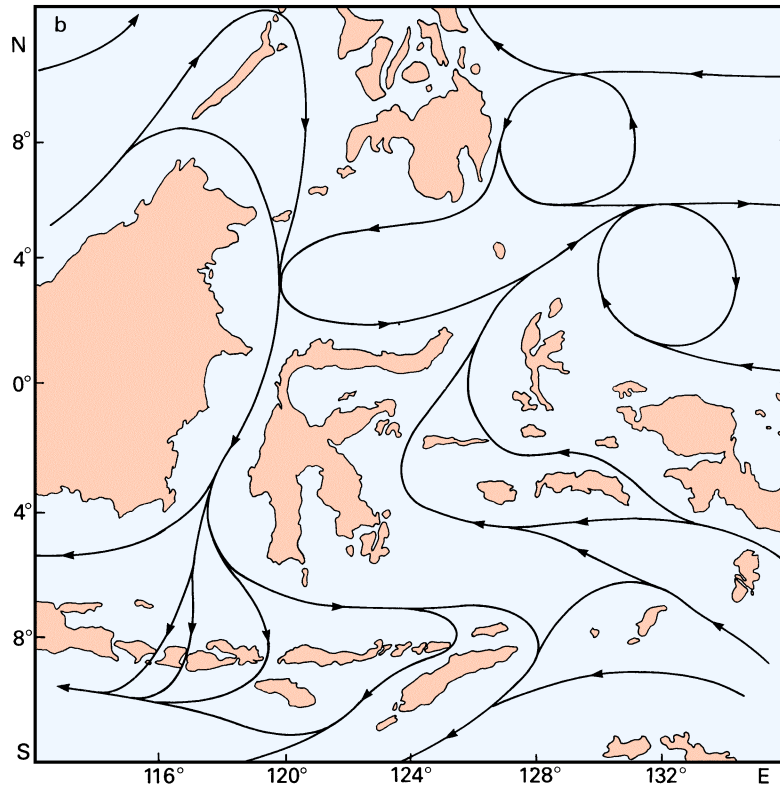
The atmospheric conditions leave no doubt that the Australasian Mediterranean Sea is a dilution basin. However, its circulation differs significantly from the schematic diagram of Figure 7.1. In the diagram, water that enters below the surface layer freshens as it is entrained into the surface layer and exits the basin with reduced salinity; deep water renewal through vertical convection is inhibited during all seasons by the high stability of the water column and is thus extremely slow, being determined by the rate of inflow over the sill. In the Australasian Mediterranean Sea, deep water renewal follows this scheme, but the circulation is markedly different. Nearly all inflow of high salinity water across the sill between the Sulawesi Sea and the Pacific Ocean proper occurs over the entire water depth, and nearly all outflow of low salinity water occurs into the Indian Ocean, again from the surface to the bottom of the passages between the south Indonesian islands. The modification is caused by the need for a net depth-integrated transport from the Pacific to the Indian Ocean. This requirement stems from the necessity to maintain constant pressure around islands. Constant pressure around Australia leads to a difference in depth-integrated steric height of about 70 m^2 between the western Australian coast (which shows the same values as the Australian east coast) and the east coast of the South Pacific Ocean. The net northward flow between Australia and Chile therefore has to pass through the Indonesian seas. Without this requirement, the freshened water would leave the Indonesian basins into both oceans - depending on the monsoon season - in a well defined surface layer.

Direct current measurements in the Australasian Mediterranean Sea are available for only a few locations and are often of short duration. The net transport is believed to be westward at all times, from the Pacific to the Indian Ocean. It occurs as a western boundary current (i.e. with highest velocities along Mindanao and Kalimantan) and is made up of two components, the surface current driven by the monsoons and the deeper reaching interoceanic throughflow. Although the wind-driven flow opposes the throughflow during May - September and follows it during November - March, the total westward transport reaches a maximum in August and goes through a minimum in February. The reason for this apparent contradiction is seen when the circulation of the Australasian Mediterranean Sea is considered in conjunction with that of the Indian and Pacific Oceans. During November - March the Equatorial Countercurrent of the Indian Ocean is fully developed, supplying water to the region where the outflow from the Australasian Mediterranean Sea occurs and raising the sea level. As a result the pressure gradient from the Pacific into the Indian Ocean is small, and the throughflow is at its minimum. During May - September the Equatorial Countercurrent in the Indian Ocean is replaced by the South Equatorial Current which expands northward under the south monsoon, drawing water away from the eastern Indian Ocean. This lowers the sea level in comparison to the Pacific Ocean and produces maximum throughflow.

First estimates for the throughflow based on geostrophic calculations from a very limited data base gave annual mean values of 2 Sv or less. More recent studies indicate that the throughflow maximum should be in the range 12 - 20 Sv, while the minimum is estimated at 2 - 5 Sv. None of these estimates are derived from direct current observations. Some are the result of numerical models of the world ocean circulation with fairly coarse resolution and are derived as balances between total Pacific and Indian Ocean transports. Others are based on Sverdrup dynamics and calculate the transport from hydrographic observations. The current is concentrated in the upper layers and decays markedly with depth, with little transport occurring below 500 m; this makes the assumption of a depth of no motion below 1000 m reasonably acceptable. Recent observations from current meters moored in the west Flores Sea and in Lombok Strait for the period January 1985 - March 1986 showed consistent flow from the Pacific to the Indian Ocean of 0.9 m s^{-1} and more during August. During October - March the flow was interrupted by frequent reversals of 10 - 20 day duration, but when it set southwestward it still attained 0.6 m s^{-1}. These and similar observations indicate that the fairly large transports inferred from numerical models and Sverdrup calculations might well be realistic. Annual mean transport through Lombok Strait works out at about 1.7 Sv, with virtually no flow during November - January, 1 Sv in February - June, and maximum transport of 4 Sv in August (Murray and Arief, 1988). Given that Lombok Strait is one of the minor passages, these figures suggest fairly large total throughflow. A recent attempt to estimate the flow through all channels into the Indian Ocean from geostrophic calculations gave a total transport of 24 Sv, again pointing towards a large throughflow .

Surface currents can reverse seasonally despite continuous net westward throughflow; this is known for Lifamatola Strait, the passage from the Molucca Sea to the Buru Basin which leads into the North Banda Sea, where the current sets northward during August but southward during February. A sketch of the surface circulation constructed to the best of available knowledge is given in Figure 13.6.

Currents below 500 m depth are even less well surveyed than upper layer currents. Estimates from geostrophic calculations indicate concentration of the flow in the upper few

hundred meters (18 Sv or $^3/_4$ of the total transport of the estimate mentioned above were found in the layer 0 - 150 m). The few observations that are available show, however, that surprisingly large velocities do occur close to the ocean floor at some locations. Current meters moored in Lifamatola Strait during January and February of 1985 in 1940 m water depth gave mean speeds of 0.61 m s^{-1} about 100 m above the bottom and 0.40 m s^{-1} about 400 m above the bottom. At both depths the currents regularly exceeded 1 m s^{-1} during spring tides. Such large velocities have to be associated with strong mixing. This will become evident in the discussion of bottom water renewal below.
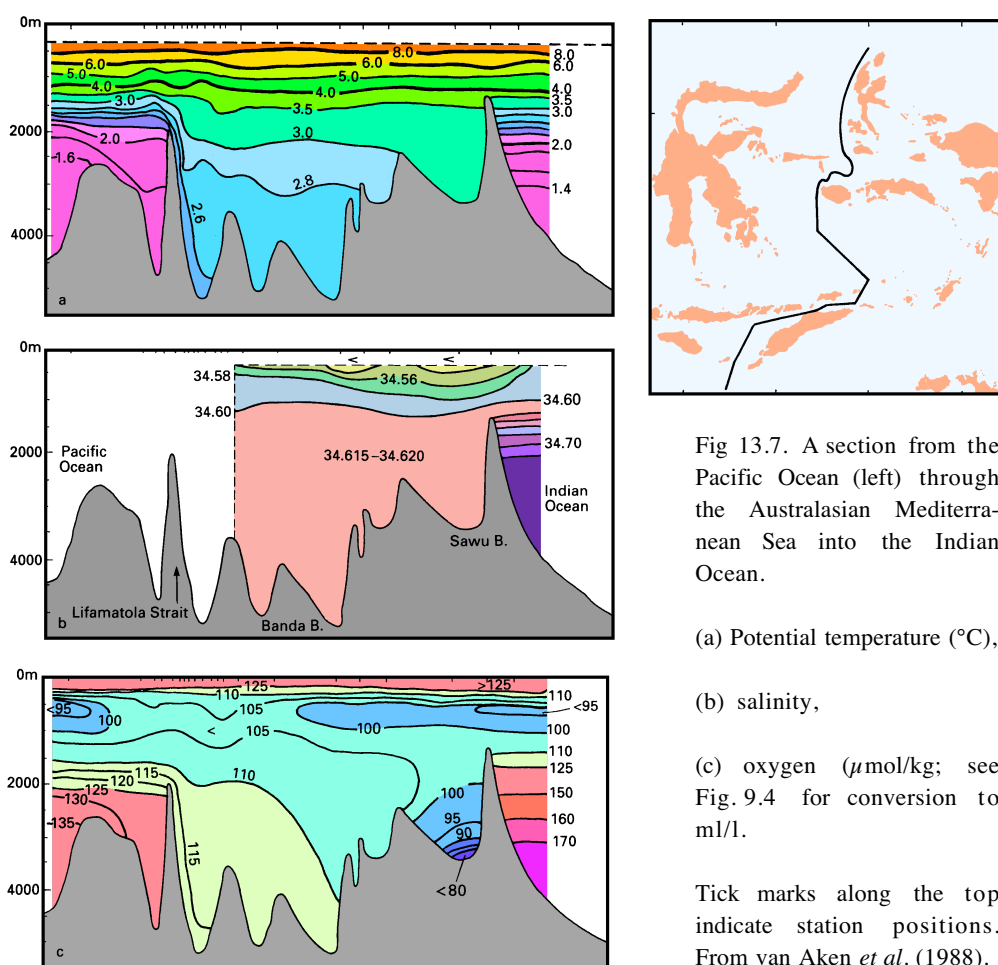
Fig 13.7. A section from the Pacific Ocean (left) through the Australasian Mediterranean Sea into the Indian Ocean.

(a) Potential temperature (°C),

(b) salinity,

(c) oxygen (μmol/kg; see Fig. 9.4 for conversion to ml/l.

Tick marks along the top indicate station positions. From van Aken *et al.* (1988).

Figure 13.7 gives a hydrographic section from the Pacific Ocean north of Halmahera through the Molucca, Banda and Sawu Seas into the Indian Ocean south of Timor, obtained during one of the rare expeditions into the region. Unfortunately no salinity data were obtained on the Pacific side, so the character of the Australasian Mediterranean Sea as a dilution basin between the two oceans does not come out as clearly as it could. However, salinity in the Banda Basin is seen to vary by less than 0.06 over the entire water column, and lowest salinities are found in the Sawu Sea. The effect of freshwater input at the surface comes out more clearly in a comparison of T-S diagrams along the path of the throughflow (Figure 13.8) which shows that the vertical salinity gradient of the Pacific Central Water virtually disappears during the passage through the Indonesian seas. Mixing with Indian Central Water restores the gradient and brings the T-S diagram nearly back to its original form. This water mass conversion affects the upper 1000 m of the water column, despite the fact that adding freshwater at the surface increases the stability. Turbulent mixing must therefore occur over a large depth range and must be able to overcome the strong density gradient. Indications for strong mixing at great depth can be seen at sills such as Lifamatola Strait. Figure 13.7 shows that the water that fills the Buru and Banda basins is drawn from about 1500 m depth some 500 m above the sill depth, indicating that strong bottom currents of probably tidal character are able to mix the water over some hundreds of meters. Support for this conclusion comes from the oxygen data (Figure 13.9) which indicate an oxygen maximum above the sill as a result of downward mixing of water from above.
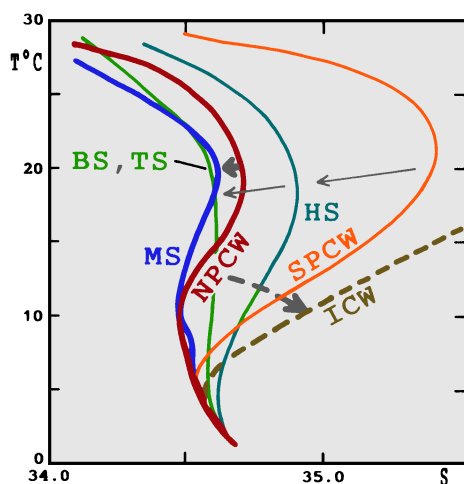
Fig. 13.8. Temperature-salinity diagrams along the path of the Indonesian through-flow, showing the transformation of Pacific Central into Australasian Mediterranean Water (demonstrating the character of the Australasian Mediterranean Sea as a dilution basin) and subsequently into Indian Central Water. South Pacific Central Water (SPCW) passes through the Halmahera Sea (HS) into the South Banda (BS) and Timor Seas (TS). North Pacific Central Water (NPCW) passes through Makassar Strait (MS) to the Timor Sea (TS). Both are then converted into Indian Central Water (ICW). Adapted from Ffield and

The mixing process in the upper 1000 m of the Australasian Mediterranean Sea is unique since it achieves nearly complete homogenization of the salinity field without destroying

the temperature stratification. This excludes deep vertical convection as the main mixing agent and requires highly turbulent flow well below the layer affected by the wind. Most likely the turbulence is concentrated near sills and related to strong tidal currents. The turbulence does, of course, affect salinity and temperature in identical fashion, so different surface boundary conditions for salinity and temperature are required to erase a salinity gradient without eliminating the temperature gradient. While a high freshwater input at the surface is responsible for homogenizing the salinity, maintaining the temperature gradient in the presence of strong mixing is impossible without a large input of heat to keep the sea surface temperature up. The atmospheric conditions found in the Australasian Mediterranean Seas can thus be deduced from its T-S properties.
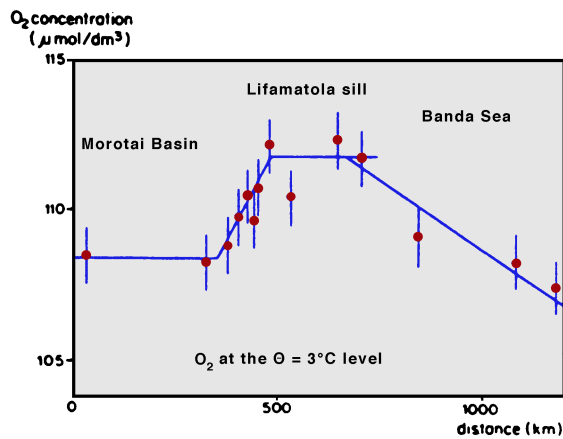
Fig. 13.9. Oxygen (units see Fig. 13.7) at the level of the 3°C potential temperature isotherm in Lifamatola Strait. From van Aken et al. (1988).

The turbulence of the upper layer does not reach much below the sill depths of the various basins. Nevertheless, oxygen values in the deep basins do not differ dramatically from those of the waters above, indicating reasonably short renewal times for the water below the sill depths. Figure 13.10 gives renewal paths and age estimates for bottom water derived from the distribution of dissolved silica. Most of the water participates in the interoceanic throughflow and has transit times of a few years. Water movement through the Seram Sea is from the east, partly in continuation of a loop from Makassar Strait through the South Banda Sea, partly as inflow from the Indian Ocean. The oldest water in the region is probably found towards the end of the loop in the deep depression of the South Banda Sea below 7000 m (the Weber Deep).
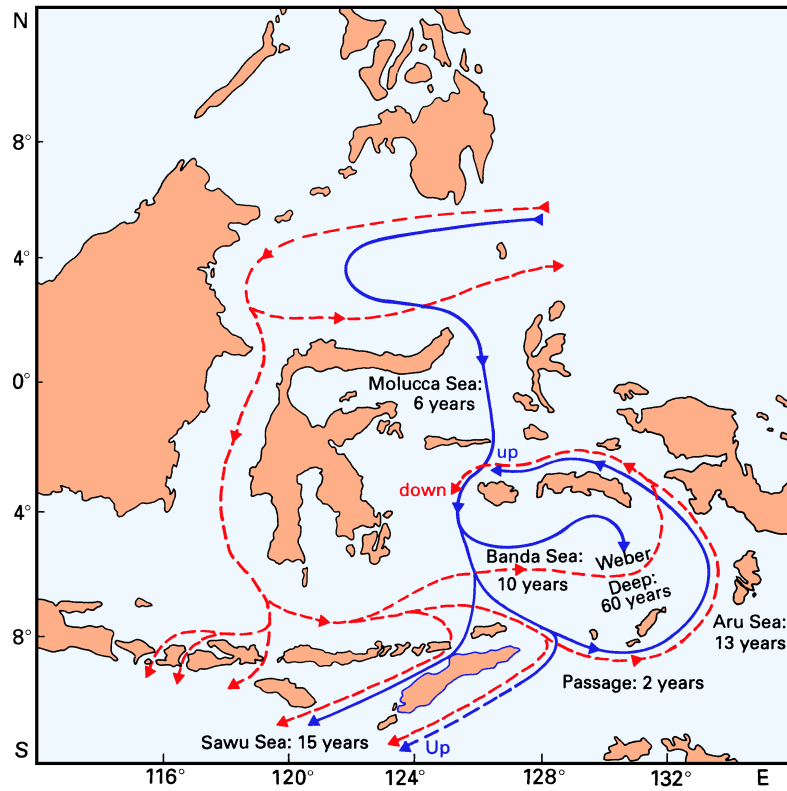
Fig. 13.10. Sketch of intermediate (broken lines) and deep water movement (full lines). Estimated transit times of bottom water are also indicated. Adapted from van Bennekom (1988).